POSSIBILITY OF ACHIEVING AN ACCEPTABLE RESPONSE RATE OF GAS-FILLED SURGE ARRESTERS BY SUBSTITUTION OF ALPHA RADIATION SOURCES BY SELECTION OF ELECTRODE MATERIAL AND THE ELECTRODE SURFACE TOPOGRAPHY

by

Dalibor S. ARBUTINA [1], ***Aleksandra I. VASIĆ-MILOVANOVIĆ*** [1], ***Teodora M. NEDIĆ*** [2], ***Aco J. JANIĆIJEVIĆ*** [2], ***and Ljubinko B. TIMOTIJEVIĆ*** [2]

[1] Faculty of Mechanical Engineering, University of Belgrade, Belgrade, Serbia
[2] Faculty of Technology and Metallurgy, University of Belgrade, Belgrade, Serbia

Scientific paper
https://doi.org/10.2298/NTRP2003223A

The possibility of substituting the usage of a radioactive α-source to improve the characteristics of the gas surge arrester is considered in this paper. The solution to this problem is sought in the engineering of the characteristics by applying different electrode materials and varying electrode surface topography. Materials that differ in the output work value were examined. The electrode surface topographies were either polished, or with engraved regular spikes, or with polished cavities. The paper is mostly experimental in nature. The experiments were performed under well-controlled laboratory conditions. The measurement uncertainty of the experimental procedure was satisfactory. Experimental results were processed by sophisticated statistical methods of low statistical unreliability. The obtained results show that it is possible to avoid the installation of a radioactive source in the gas surge arresters and how it should be done. In this way, a possible contamination of the natural environment with extremely dangerous α – radioactive sources would be avoided.

Key words: gas-filled surge arrester, insulation co-ordination, low voltage level

INTRODUCTION

The development of semiconductor components of a multilayer structure and their miniaturization results in a significant reduction in their durability. The reduction in the durability of semiconductor components with a high degree of miniaturization is most pronounced in relation to the occurrence of overvoltage. The reason for this is a significant reduction in the thickness of the insulation layers. For that reason, more and more attention has been dedicated to overvoltage protection, *i*. *e*. co-ordination of insulation at a low voltage level [1, 2].

The co-ordination of insulation at a low voltage level should protect electronic components, and assemblies, from the occurrence of overvoltage in the network. The overvoltage in the network can be of atmospheric or commutational origin [3, 4]. The overvoltage of atmospheric origin has a rise time of the order of microseconds, and overvoltages of commutation origin have a rise time of the order of milliseconds.

* Corresponding author; e-mail: teodora.nedic@nuklearniobjekti.rs

In addition to overvoltage of atmospheric and commutation origin, there is the possibility of induced overvoltage due to, hopefully unlikely, the explosion of a nuclear bomb in the atmosphere. Such voltages would be characterized by a rise time of the order of nanoseconds and would be induced in all wire structures of the electronic components or the assemblies.

In laboratory practice, the overvoltages are simulated by so-called double-exponential impulses, which are characterized by a rise time and a fall time [5, 6]. Drain diodes, varistors, and gas surge arresters are used as components for electronic components protection [7, 8]. All these components have such characteristics that up to a certain voltage value they have a very high (theoretically infinite) resistance, and after that value, they have a very small (theoretical zero) resistance. With such characteristics, the overvoltage protection components are connected in parallel to the protected electronic component, or assembly, and so connected should conduct a voltage, higher than the nominal, to the mass. In addition to the above-mentioned characteristics of the overvoltage protection components, they shouldn't capacitively or inductively load the electronic component or assembly which they protect. In addition

to all the above characteristics of the components for the overvoltage protection, the most important are the response speed time, stable conditioning, and the possibility of a larger number of triggers without the occurrence of irreversible changes in characteristics. In practice, the components for the overvoltage protection partially and differently accomplish these conditions [9-13].

The drain diodes have characteristics similar to the Zener diodes. They have the best response speed of all overvoltage protection components, do not load the capacitively or inductively protected component, or assembly. They are always conditioned. Their disadvantage is that they are destroyed by higher values of the overvoltage power that they drain [14, 15].

The current-voltage characteristic of the varistor is significantly worse than the corresponding drain diodes characteristics. The varistor also does not load the capacitively and inductively protected element, or assembly. During multiple processing, minimal irreversible changes in the characteristics of the varistor have been observed. The varistor is always conditioned. Their response time is longer than the drain diode response time. The varistor can conduct an overvoltage of higher power than the drain diode, but at high overvoltage powers, it leads to permanent damage or destruction [16, 17].

The gas-filled surge arrester (hereinafter GFSA) has a weaker current-voltage characteristic than the varistor. The GFSA minimally loads the capacitively protected component, or assembly, but does not load it inductively. Significant irreversible changes in GFSA characteristics occur during multiple processing. After a time of several hours, GFSA is deconditioned. Its response time is significantly longer than the response time of the drain diodes and varistors. The GFSA can take overvoltages of almost unlimited power. This last feature of GFSA makes them indispensable components for overvoltage protection. The GFSA are used either separately or in hybrid combinations with the other overvoltage protection components [18-21].

Since the overvoltage protection components have good and bad properties, a lot of effort has gone into improving their characteristics. The GFSA have been most commonly tested to improve their characteristics. One of the solutions, which significantly contributed to the acceleration of the GFSA response, is the insertion of a radioactive α – source into its interior. However, this solution has a serious environmental shortcoming since its application introduces a large number of components into the environment with built-in radioactivity that is impossible to control, monitor, and properly dispose of. The aim of this paper is to examine the possibility of radioactive α – source substitution in GFSA by the choice of electrode materials and the manner of their surface treatment [22-25].

THE GAS-FILLED SURGE ARRESTERS

The GFSA works on the principle of electrical breakdown of gases. Structurally GFSA consists of two gaseous isolated electrodes. One electrode is banded for a point protected from overvoltage and the other one is grounded. The GFSA electrodes provide a homogeneous electric field (they are often made in the Rogowski cloud to avoid the edge effects). The electrodes are usually made of tungsten because it has a favorable ratio of melting temperature and thermal conductivity. Noble gases are used as an insulating gas (in German-speaking areas they are called fuses with noble gas) [26, 27].

The noble gas in GFSA is under pressure. The chamber containing the electrodes and the noble gas must be well sealed as the noble gases are monoatomic and they could easily diffuse from the chamber (regardless of whether they are under pressure). Since the law of similarity is indisputably valid for such a configuration, the working point is determined by the product of pressure p and interelectrode distance d (on the abscissa) and nominal voltage (DC breakdown voltage on the ordinate) [28, 29].

The GFSA working point is set near the Paschen minimum on the Paschen's curve. It is usually placed at points to the right of the minimum where the breakdown has occurred by a streamer mechanism. Recently, it has been suggested to place the GFSA working point at points to the left of the minimum at which the breakdown takes place by an abnormal Paschen mechanism. This second solution provides greater stability of the working point in a longer period of exploitation [30, 31].

ELECTRICAL BREAKDOWN MECHANISM

The electrical breakdown of gases is divided according to the shape of the applied voltage into DC, AC, and impulse breakdown. Based on the mechanism by which the breakdown takes place, it is divided into the Tausend's and the streamer's mechanism (there are also some combinations of breakdown mechanisms, such as the mentioned abnormal Paschen's mechanism). As regards GFSA functioning, the DC and the impulse types of breakdowns are interesting, as well as both breakdown mechanisms [32].

The DC breakdown of gases is achieved by increased DC voltage whose rise time is significantly longer than the time characteristic for the elementary processes of the electrical discharges in gases. The DC breakdown voltage value is a deterministic magnitude (when measuring the measurement uncertainty type A is zero). The DC breakdown voltage can be numerically calculated for a certain electronic configuration and for certain gas pressure. The impulse gas break-

downs are achieved by a DC impulse voltage whose rise time is of the same order of magnitude as the time characteristic of the elementary processes of electric gas discharges. The impulse voltage breakdown value is a stochastic magnitude which, as a rule, belongs to the three-parameter Weibull distribution. In contrast to the DC breakdown voltage value, the impulse voltage breakdown value can be calculated. However, it is possible to determine the probability of a certain quintile that the impulse voltage breakdown value falls at a certain point of the voltage-time plane. This is obtained by calculating the impulse (volt-second) characteristics of the gas insulation, which are also the best indicators of the GFSA rate response [33, 34].

IMPULSE CHARACTERISTICS

The electrical breakdown of gas is a self-sustaining two-stepped process. The main condition for initiation of the electrical breakdown of gas is the appearance of a free electron in the part of the electric field in which it can assume enough energy, at one mean free length path, to ionize a neutral atom or molecule (the so-called initial electron). After the first ionization collision, an avalanche is developed, which ends with the arrival of a geometrically progressive multiplied electron beam at the anode. This completes the first stage of the electrical breakdown. The second stage is crucial. It represents the positive feedback of the first (initial) avalanche and subsequent avalanches. This so-called secondary process occurs either at the electrodes or in the gas. If secondary processes of electrical discharge in the gas occur at the electrodes, the breakdown mechanism is the Tausend type. If secondary processes of electrical discharge in the gas occur in the gas, the breakdown mechanism is of the streamer type [35].

As mentioned, in the case of the DC breakdown there are numerical algorithms that allow the breakdown voltage values to be calculated. For that purpose, it is necessary to calculate the values of the electric field and know the so-called avalanche coefficients. In the case of an impulse breakdown, this is not possible, but it is possible to determine the impulse characteristic that determines the dependence of the impulse voltage breakdown on the time of increase of the impulse voltage with the probability quantile as a parameter [36].

The impulse voltage breakdown is achieved by impulses whose rise time is the same order of magnitude as the time characteristic of the elementary processes of electrical discharge. For this reason, time affects the value of a random variable pulse breakdown voltage. Figure 1 shows the time dependence of the impulse breakdown of gas.

In fig. 1, t_S signifies the statistical time that represents the period from exceeding the DC breakdown voltage, U_B, to the appearance of the initial electron, t_L

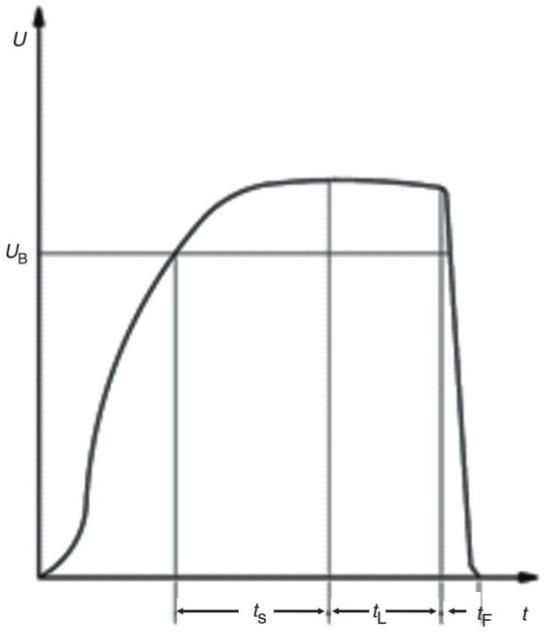

Figure 1. The impulse voltage with which the gas insulation breakdown was performed

denotes the avalanche time, *i. e*. the period that begins with the first avalanche and ends with the formation of positive feedback of the electric discharge, and t_F denotes the formative time, which indicates the period from the movement of the interelectrode rise by multiple avalanches to the spark channel thermal ionization.

In order to determine the impulse characteristic, the starting assumption is that the plasma in the intermediate electrode space moves at a speed υ that is linearly dependent on the electric field

$$\upsilon(x,t) \quad k[E(x,t) \quad E_S(x)] \tag{1}$$

where k is a factor that depends on the polarity of the voltage at the electrodes, $E_S(x)$ is the electric field that corresponds to the DC breakdown voltage, U_s. Since a homogeneous and pseudo- homogeneous electric field can be expressed as a product of two components, one of which depends on time and the other on spatial coordinates

$$[E(x.t) \quad u(t)g(x)] \tag{2}$$

inserting eq. (1) into eq. (2), the following is obtained

$$V(x,t) \quad k[u(t) \quad U_S]g(x) \tag{3}$$

After separating the variables and integration over time, the following is obtained

$$\frac{1}{k}\int_{t_1}^{t_a}\frac{\mathrm{d}v}{g(x)} \quad \int_{t_1}^{t_a}[u(t) \quad U_S]\mathrm{d}t \quad P \quad \text{const.} \tag{4}$$

where t_1 is the time after which the impulse voltage reaches the value of the DC breakdown voltage and

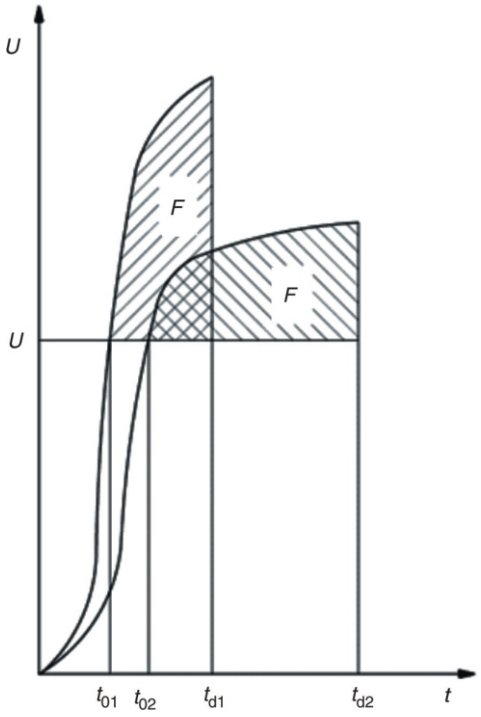

Figure 2. Schematic representation of the law of surface constancy in the voltage-time plane during the impulse breakdown

$t_1 + t_a$ is the time after which the Tausend electric discharge mechanism is changed into a streamer electric discharge mechanism. As can be seen from eq. (4) the impulse breakdown has occurred after the value of the surface P, which is constant, is reached between the impulse voltage and the line $u(t) = U_s$ [37]. Figure 2 schematically shows the law obtained by eq. (4) for two different forms of impulses.

Equation (4) is used to determine the impulse characteristics of GFSA in the following steps:

1 – Based on a large number of measurements (1000) with the same voltage form the statistical distribution of the random variable "impulse voltage breakdown" is determined.

2 – On the basis of such a statistical distribution, the quantiles of the impulse breakdown probability x and y are set (usually $x = 0.1$ % and $y = 99.9$ %).

3 – Based on the values of these quantiles, the calculated (or measured) values of U_s determine the surfaces P_X and P_Y.

4 – Based on certain values of P_X and P_Y and the law of their constancy, the random variable quantiles for arbitrary impulse voltage are determined [38].

EXPERIMENT

In order to experimentally examine the possibility of replacing the α-radioactive source in GFSA by choosing the electrode materials and the way of processing their surfaces, a chamber representing the GFSA model was used. The chamber used was also constructed in such a way that it was possible to change the electrodes, the type of gas, the gas pressure, and the interelectrode distance. The same flexible chamber was used as in the paper [39].

The flexible chamber (GFSA model) was included in the gas circuit, which enabled the adjustment of the pressure value in the working gas chamber. The pressure was set to correspond to the value at 20 °C. The multiple vacuuming and filling with working gas of the chamber guaranteed the high purity of the working gas. It was used as the working gas. The same gas circuit was used as in the paper [39].

The interelectrode distances were 0.1 mm, 0.2 mm, 0.5 mm, and 1 mm. Pressure values varied from 1 mbar to 1 bar (1 bar = 10^5 Pa). The electrode system was formed from Rogowski-shaped electrodes. In the case of measurements using a radioactive -source (^{241}Am) placed on the wall of the chamber across from the interelectrode gap. The tungsten electrodes used were the same as in the paper [39].

The DC voltage source of 8 Vs^{-1} and the impulse voltage source with a variable rise rate and amplitude significantly higher than the expected impulse voltage breakdown value (which means that the breakdown always occurred at an increasing part of the impulse voltage) were used as a voltage source. During the work, the impulses rise rates of 1 kV(μs)$^{-1}$, 2 kV(μs)$^{-1}$, 5 kV(μs)$^{-1}$, 10 kV(μs)$^{-1}$, 50 kV(μs)$^{-1}$, 100 kV(μs)$^{-1}$, and 200 kV(μs)$^{-1}$ were used. Figure 3 shows the DC voltage circuit diagram and fig. 4 the impulse voltage circuit diagram.

In order to examine the influence of the electrode material on the GFSA characteristics, electrodes made of either an electron alloy or aluminum, or silver, or iron, or tungsten (of course without a radioactive source) were used. Also without a radioactive source, and in order to examine the influence of electrode surface treatment on GFSA characteristics, tungsten electrodes were used whose surfaces were either polished to a high gloss, or sandblasted, or with engraved regular pyramids 325 μm high, or with cavities of a 100 μm radius.

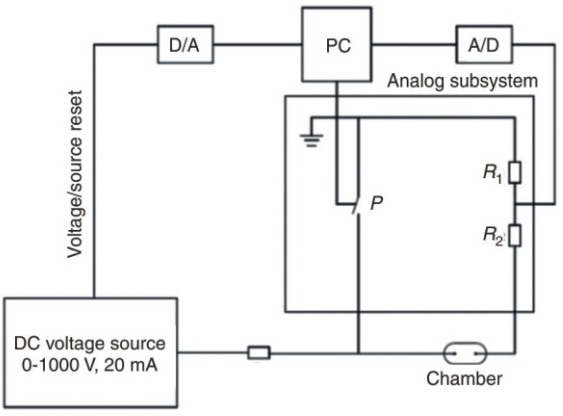

Figure 3. Diagram of the used DC voltage circuit

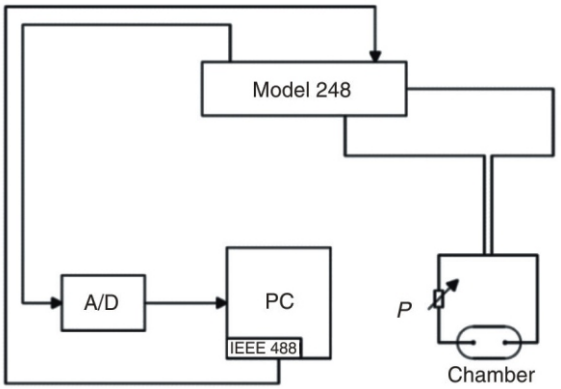

Figure 4. Scheme of the used impulse voltage circuit

Figure 5 shows the electrode surface with engraved pyramids, and fig. 6 shows the surface of the electrode with cavities.

The measuring procedure consisted of the following steps:

1 – Adjustment of the interelectrode distance and pressure (*i. e*. adjustment of the working point).

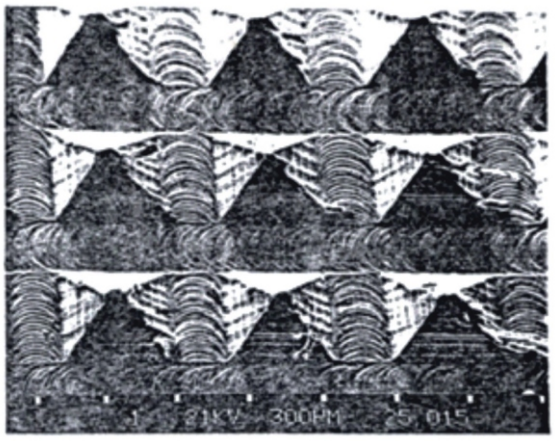

Figure 5. The electrode surface with engraved pyramids

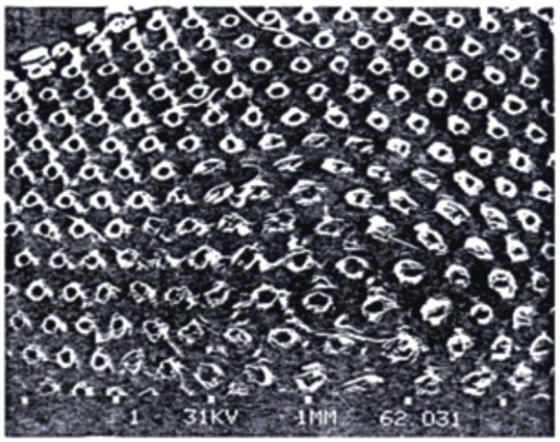

Figure 6. The surface of the electrode with cavities

2 – The measurement of 50 values of DC breakdown voltage with pauses between two consecutive breakdowns of 30 seconds.

3 – The measurement of 1000 values of impulse voltage breakdown with all rise rates of impulse voltage.

4 – Change of the working point and repetition of the procedure (after the end of the series of measurements, the measurement is repeated with another pair of electrodes). The combined measurement uncertainty was less than 8 % [40].

The processing of the experimentally obtained results consisted of the following steps:

1 – Elimination of suspicious measurement results using Chauvenet's criterion.

2 – Testing of an experimentally obtained random variable "impulse voltage breakdown" with a unique statistical sample using a *U*-test.

3 – Determining the affiliation of experimentally obtained random variables to the Normal distribution or to one of the distributions of the minimum value by the graphical method and the χ^2 test.

4 – Determining the central moments of the obtained distribution (which best fits the obtained results).

5 – Determination of the probability quantile of 0.1 % and 99.9 % of the obtained distribution.

6 – Drawing Pashen's curves and the impulse characteristics.

RESULTS AND DISCUSSION

Figures 7 and 8 show the results of the *U* – test for a random variable the impulse voltage breakdown at a product value of 100 mbar mm obtained by an im-

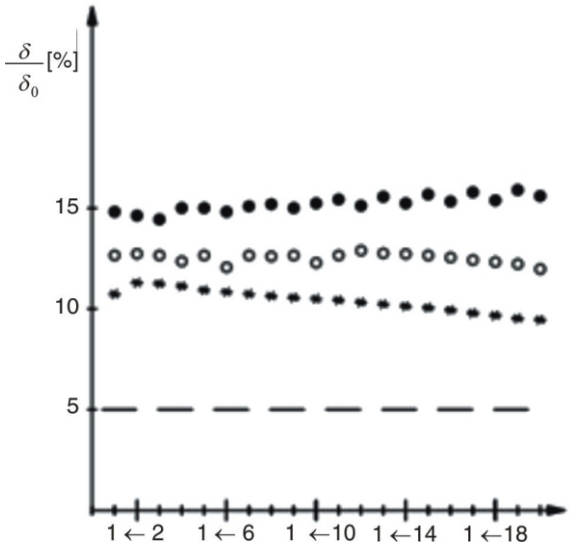

Figure 7. The *U*-test results for the random *variable impulse voltage breakdown*, copper electrodes + α – source, ○ tungsten electrodes, * copper electrodes, impulse rise rate of 10 kV(μs)$^{-1}$, – 5 % statistical unreliabil-

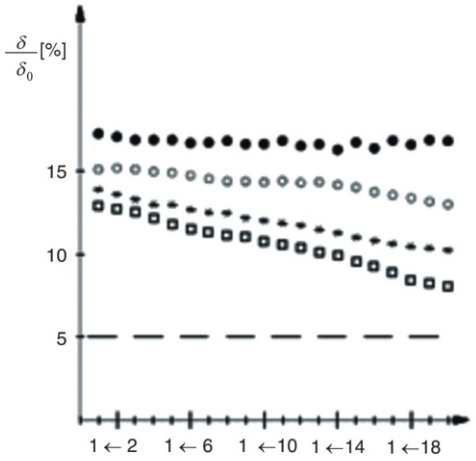

Figure 8. The *U*-test results for the random variable *impulse voltage breakdown*, ● copper electrodes + α – source, ○ silver electrodes, * aluminum electrodes, □ electron alloy electrodes, – 5 % statistical unreliability

pulse rise rate of 10 kV(μs)$^{-1}$. The variable parameters of the experiment were: the electrode system with and without an – radioactive radiation source, different electrode materials, and different interelectrode distances (with product *pd* = const.). During the experiment, no influence of the presence of the radioactive α – source on the stability of the random variable statistics of *impulse voltage breakdown* was observed.

The results shown in figs. 7 and 8 show that the random variable *impulse voltage breakdown* and its affiliation with a unique statistical sample is affected by the electrode material (at a constant impulse rise rate). Although all random variables in figs. 7 and 8 belong to a unique stochastic distribution (with 5 % statistical unreliability), the trends of this affiliation differ for different materials. This change in trends is least pronounced in the case of tungsten, and most pronounced in the case of electrons. Based on that, it can be concluded that, in this case, the decisive values are the melting point of the material, and its thermal conductivity. Namely, materials with a high melting point and high thermal conductivities (tungsten), suffer minor changes in the electrode topography, and less when the electrode material is ejected into the interelectrode space (by the explosion of the spark channel). For this reason, it comes to a less irreversible change in insulation (electrode system + insulating gas), so there is less influence on the statistical error of the random variable *impulse voltage breakdown*. In the case of materials with a lower melting temperature and lower values of thermal conductivity, the changes in insulation after multiple breakdowns are significant, which results in a greater influence on the statistics of the random variable *impulse voltage breakdown*.

Figure 9 shows the results of the *U*-test for the random variable the *impulse voltage breakdown* at a product value of *pd* 100 mbar mm obtained by differ-

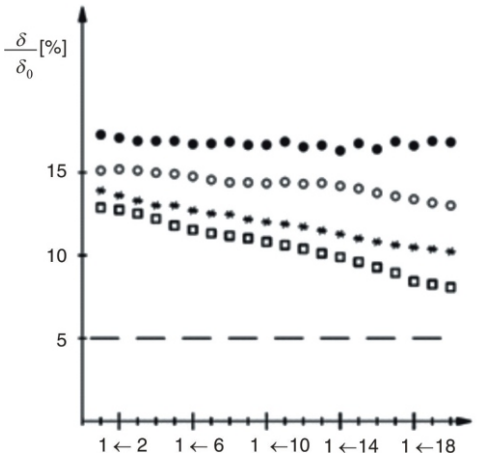

Figure 9. The *U*-test results for different impulse rates, ● copper electrodes + α – source with impulse rate of 10 kV(μs)$^{-1}$, ○ copper electrodes with impulse rate of 50 kV(μs)$^{-1}$, * copper electrodes with impulse rate of 100 kV(μs)$^{-1}$, □ copper electrodes with impulse rate of 200 kV(μs)$^{-1}$, – 5 % statistical unreliability

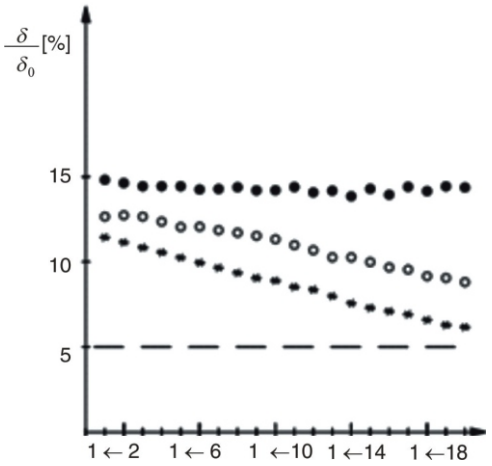

Figure 10. The *U*-test results for the random variable *impulse voltage breakdown*, ● copper electrodes + α – source of the impulse, ○ copper electrodes with engraved spikes, * copper polished electrodes, impulse rate of 10 kV(μs)$^{-1}$, – 5 % statistical unreliability

ent values of the impulse voltage rise rates. The applied experimental parameters were the same as for the results shown in fig. 8. Figure 10 shows the results of the *U* – test for the random variable of *impulse voltage breakdown* at a product value of pd 100 mbarmm obtained by impulse rate of 10 kV(μs)$^{-1}$. The variable parameters of the experiment were: an electrode system with and without an α – source of radioactive radiation, different electrode surface topographies and, different interelectrode distances (with product *pd* = const.).

The results represented in fig. 9 show that the electrode material and the presence of a radioactive source of α-radiation when the rise rate of the pulse voltage has changed, have an influence on the random variable *impulse voltage breakdown* and its belonging to a unique sample. In this respect, the electrode sys-

tem with a radioactive source of α – radiation shows the least changes. Such an electrode system is practically independent of the impulse voltage rise rate. The electrode material at lower impulse voltage values affects so that the most stable statistical random variable is *impulse voltage breakdown* in the case of electron alloy electrodes, and the most unstable is in the case of tungsten electrodes. This dependence is in very good correspondence with the value of the output work of the electrode material (electron 1.8 eV; aluminum 3.74 eV; silver 4.47 eV and tungsten 4.5 eV). This result is explained by the higher concentration of free electrons (potentially initial) in the case of the presence of a radioactive α – source and electrode material with a lower value of the output work (which such electrodes emit by the cold emission mechanism). As the concentration of free electrons formed by ionization of gas by α – particles does not depend on the impulse voltage rise rate, so the stability of the statistical variable *impulse voltage breakdown* does not depend on it. However, cold electron emission is a process that occurs in real-time and at high impulse rise rates cannot affect the stability of the statistical random variable *impulse voltage breakdown* .

Regarding the influence of the change of the interelectrode distance, at a constant value of the product pd, in the experiments whose results are shown in figs. 7-9 it is not a noticeably significant influence on the stability of the statistical random variable *impulse voltage breakdown* . This confirms the assumption of the validity of the law of similarity for the electrical discharges in gases in experiments whose results are shown in the mentioned figures.

Figure 10 shows the results of the *U* – test for the random variable impulse voltage breakdown at a product value of pd 100 mbar mm obtained by different values of the impulse voltage rise rate. The variable parameters of the experiment were the same as for the results shown in fig. 9. During the experiment, no influence of the presence of the radioactive α – source on the stability of the random variable statistics of *impulse voltage breakdown* was observed.

The results shown in fig. 10 show that the random variable *impulse voltage breakdown* and its affiliation with a unique sample are not affected by the electrode surface topography, nor by the presence of thea α – radioactive source. Figure 10 shows that the electrode surface topography affects the stability of the statistics of the random variable *impulse voltage breakdown* only in the case of electrodes with polished surfaces. The reason for that are the multiply effects of the spark on such electrodes, and thus the insulation characteristics. Figures 11(a) and 11(b) show the changes in such electrodes, *i*. *e*. fig. 11(a) the crater's appearance (polished electrodes) and fig. 11(b) the melting of spikes (electrodes with engraved spikes).

The results shown in fig. 12 show that the random variable *impulse voltage breakdown* and its be-

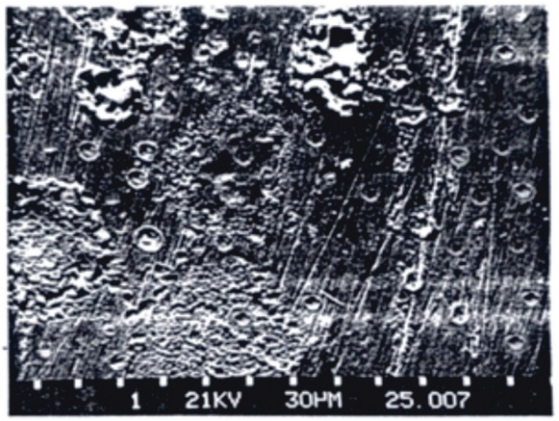

Figure 11(a). The changes in polished electrodes and the crater's appearance

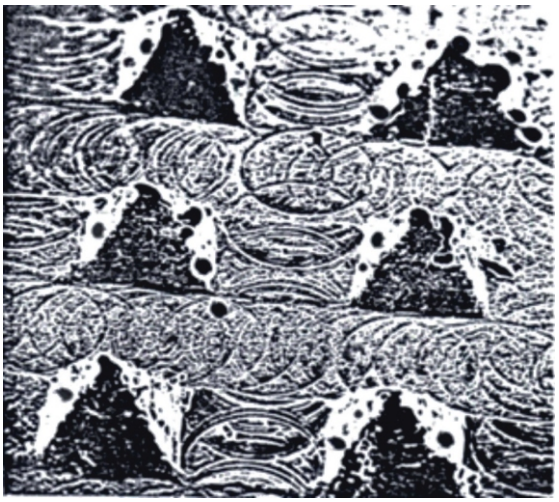

Figure 11(b). The changes in electrodes with engraved spikes and melting of spikes

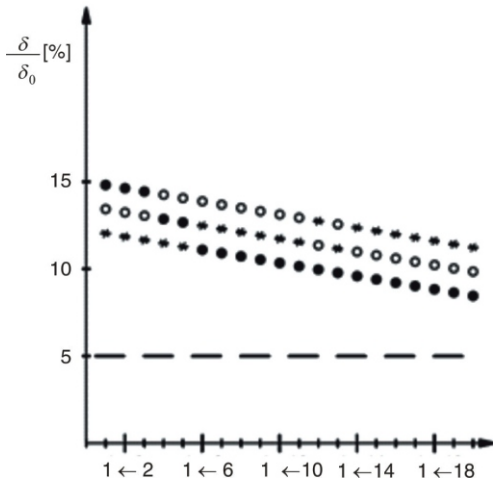

Figure 12. The *U*-test results for the random variable *impulse voltage breakdown*, • copper electrodes + α – source of the impulse, ○ copper electrodes with engraved spikes, * copper polished electrodes, – 5 % statistical unreliability

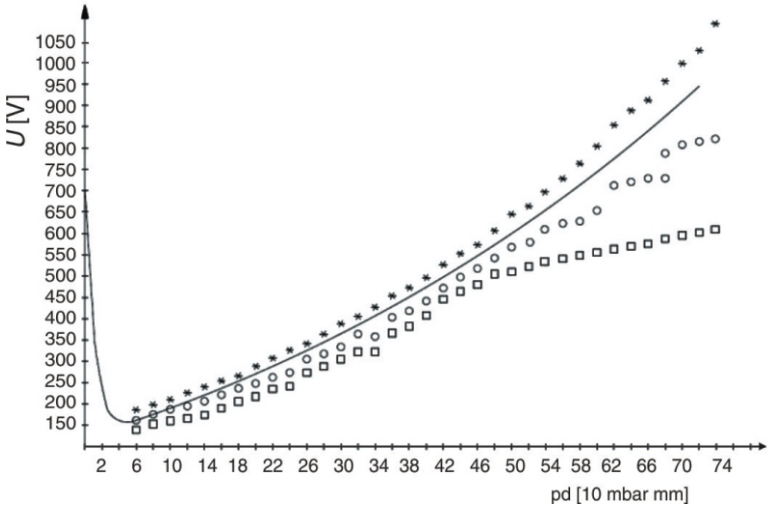

Figure 13. Experimentally determined points of the Paschen curve and theoretically calculated Paschen curve according to Tausend's criterion; * iron electrodes ○ aluminum electrodes, □ electron alloy electrodes

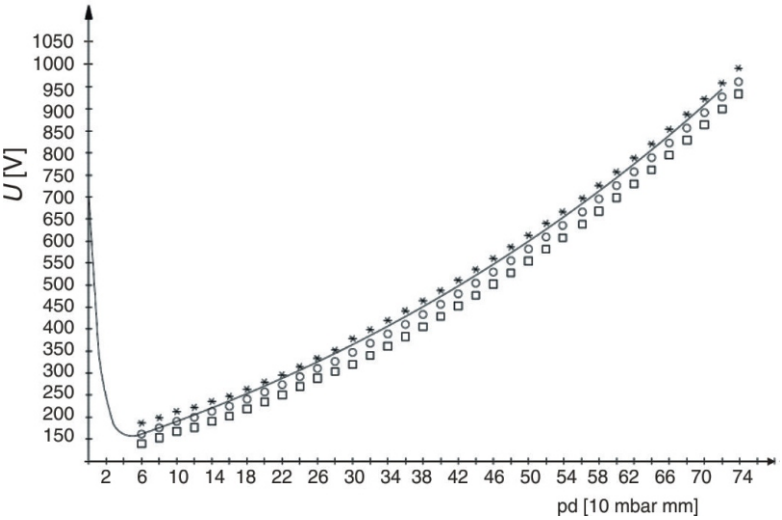

Figure 14. Experimentally determined points of the Paschen curve and theoretically calculated Paschen curve according to Tausend's criterion, * polished electrodes, ○ sandblasted electrodes, □ electrodes with cavities, – theoretically calculated Paschen curve

longing to a unique sample are affected by the electrode surface topography, and the presence of an α – radioactive source when changing the impulse voltage rise rate does not. This result can be explained by the independence of the time of the gas ionization process by α – particles and the cold emission process (in the case of engraved pyramids) and the hollow cathode effect (in the case of electrodes with cavities) in real-time. It was also found that increasing the interelectrode distance with a constant value of the product pd significantly affects the stability of the statistical random variable *impulse voltage breakdown* in the case of electrodes with cavities. This result is a consequence of the hollow cathode mechanism which ceases if the mean free length of the electron is of the order of the magnitude of the cavity radius.

Figure 13 shows the experimentally determined points of the Paschen curve obtained by DC voltage. The parameter of the experiment was the electrode material. Electron, aluminum, and iron alloy electrodes were used. Figure 14 shows the experimentally determined points of the Paschen curve obtained by DC voltage. The parameter of the experiment was the manner of processing the electrode surfaces. Copper electrodes polished to a high gloss, or sandblasted, or with cavities were used. For the results shown in fig. 13 and 14, measurements were performed with different values of the interelectrode distance with a constant value of the product *pd*.

The results shown in figs. 13-14 show that the DC voltage breakdown value for materials with a lower value of output work is lower than the DC voltage breakdown value for materials with a higher value of output work. This result can be explained by the influence of the value of output work on the secondary effects on the electrodes. Namely, the recording points are close to the minimum of the Paschen curve in which the DC breakdown is expected to take place (at least partially) by the Tausend mechanism. As the Tausend mechanism is characterized by secondary effects active on the electrodes, it is to be expected that their number is higher for materials with a lower value of the output work. In the mathematical model, this phenomenon is equivalent to an increase in the coefficients of secondary gamma emission (number of free electrons emitted from the cathode per one primary avalanche).

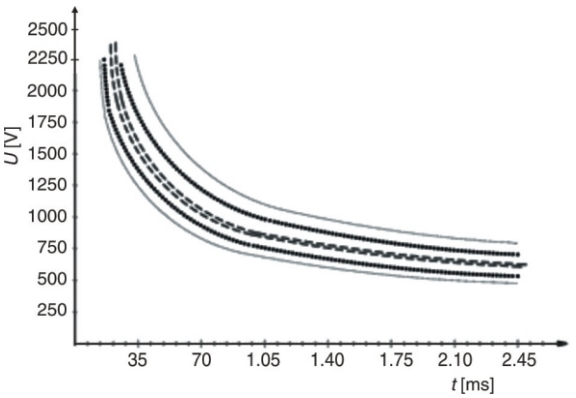

Figure 15. The impulse characteristics obtained by the law of surface constancy based on voltage measurements with a rise rate of 5 kV(μs)$^{-1}$, *pd* = 200 mbar mm, – chamber with an α – source, * electrodes made of an electron alloy, — tungsten electrodes

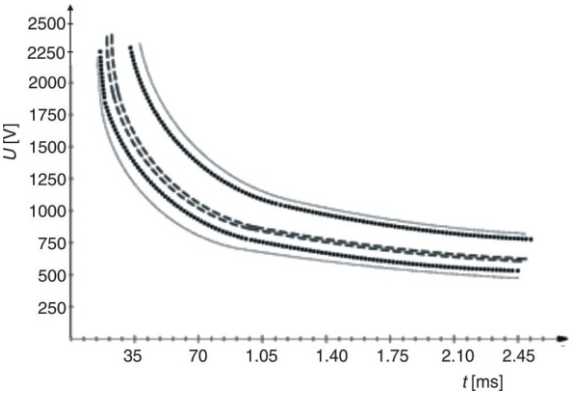

Figure 16. The impulse characteristics obtained by the law of surface constancy based on voltage measurements with a rise rate of 200 kV(μs)$^{-1}$, *pd* = 200 mbar mm, – chamber with α – source, * electrodes made of an electron alloy, – tungsten electrodes

The results shown in fig. 14 demonstrate the relative independence of the DC voltage breakdown value from the electrode surface topography. This result can be explained by the independence of the secondary processes active on the electrodes from the electrode surface topography.

Figure 15 presents the impulse characteristics obtained by an impulse voltage rise rate of 5 kV(μs)$^{-1}$ for a *pd* value of 200 mbar mm. The variable parameters of the experiment were: chamber with an α – radiation source (copper electrodes), electrodes made of an electron alloy, and tungsten electrodes. Figure 16 presents the impulse characteristics obtained by an impulse voltage rise rate of 200 kV(μs)$^{-1}$ for the same experimental parameters.

The results shown in fig. 15 indicate that the impulse characteristics obtained by using a radioactive source of α – radiation are the best from the aspect of the GFSA application. Namely, they are the longest and they grow least at the high rise rate impulses. The impulse characteristics obtained by using electrodes made of an electron alloy are, according to the previous criterion, better than the impulse characteristics obtained by using tungsten electrodes. This result indicates that the shape of the impulse characteristics mostly depends on the statistical time (which is the shortest in the case of the presence of an α – sources in the chamber). Since the lower value of the output work of the electron alloy contributes to a higher concentration of free electrons (potentially initial), the impulse characteristics obtained by using these electrodes have better characteristics than the impulse characteristics obtained by using tungsten electrodes, which have a significantly higher value of the output work. The results shown in fig. 16 point out that the difference between the impulse characteristics obtained by using electrodes made of an alloy and tungsten decreases. This can be explained by the fact that the cold emission process takes place in real-time and that there is no effect for very fast impulses.

Figure 17 shows the impulse characteristics obtained by the impulse voltage rise rate of 5 kV(μs)$^{-1}$ for a *pd* value of 200 mbar mm. The variable parameters were: a chamber with an α – radiation source, electrodes with polished surfaces, electrodes with engraved spikes, and electrodes with cavities. Figure 18 shows the impulse characteristics obtained by an im-

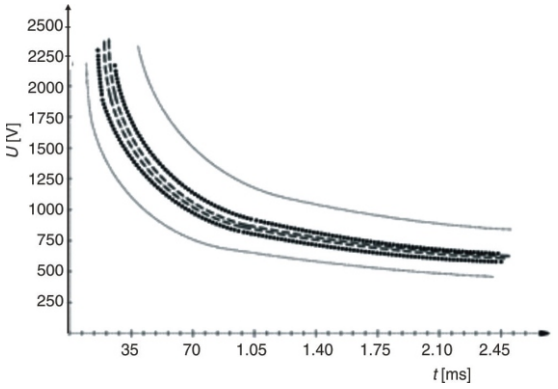

Figure 17. The impulse characteristics obtained by the law of surface constancy based on voltage measurements with a rise rate of 5 kV(μs)$^{-1}$, *pd* = 200 mbar mm, – chamber with an α – source, * electrode with cavities, – electrodes with engraved spikes

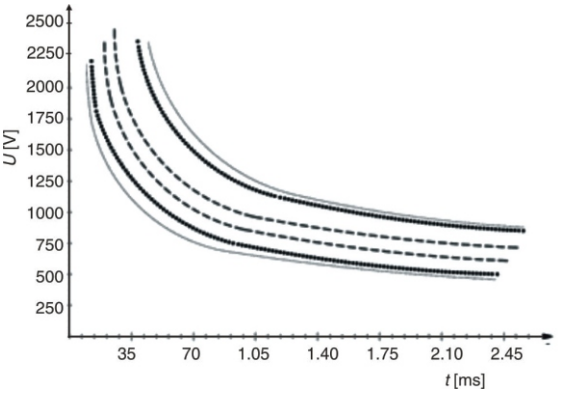

Figure 18. The impulse characteristics obtained by the law of surface constancy based on voltage measurements with a rise rate of 200 kV(μs)$^{-1}$, *pd* = 200 mbar mm, – chamber with an α – source, * electrode with cavities, – electrodes with engraved spikes

pulse voltage rise rate of 200 kV(μs)$^{-1}$ for the same experimental parameters.

The results shown in fig. 17 demonstrate that the electrode surface topography significantly affects the impulse characteristics. Very good impulse characteristics obtained by electrodes with engraved spikes and electrodes with cavities confirm that the spike effect and the hollow cathode effect significantly increase the concentration of free electrons in the interelectrode space, which affects the shortening of the statistical time. It should be noted that the effects obtained by electrodes with engraved spikes and cavities lag behind the effect achieved by the source of α – radiation, but not so much that they should not be considered as alternatives. The results shown in fig. 18 show that the efficiency of the spike and hollow cathode effect decreases with an increasing impulse rate. This is explained by the already mentioned finite time required for the development of the spike and hollow cathode effects. It should be noted that the same experiments were performed with a changed interelectrode distance with the same value of the product *pd*. These experiments showed a weakening of the efficiency of the spike effect and the hollow cathode effect with increasing interelectrode distance. Based on that, it can be concluded that the law of similarity for the electrical discharges in gases does not apply to the consideration of the influence of the electrode surface topography on the impulse breakdown of gas.

CONCLUSIONS

According to the results presented in the paper, it can be concluded that it is possible to achieve a significant improvement of the GFSA impulse characteristics by engineering the electrode material and the electrode surface topography. This improvement is achieved by a positive synergy of the output work values, spike effect, and hollow cathode effect. However, it was found that such engineering characteristics of the GFSA without the use of a radioactive source of α – radiation can almost be equated with the characteristics of the GFSA with a radioactive source of α – radiation only in the case of protection against the commutation overvoltages. In the case of protection against atmospheric overvoltages, the GFSA with a radioactive α – source show a certain, though not drastic, advantage. For very fast overvoltages, the origin of a nuclear explosion in the atmosphere, the proposed engineering does not have any substantial effects. In that case, the solution with an α – radioactive source is much more efficient, but it does not provide the required level of protection. This result is explained by the finite time characteristic of the cold emission effect and the hollow cathode effect. However, the conclusion is that the overvoltage protection in the worst-case scenario (extremely fast overvoltages) cannot be effective and that the discrete electronic components (much more resistant to overvoltages) should be used to make electronic circuits that must function under such conditions. In this way, the use of radioactivity in the construction of the GFSA could be completely rejected.

ACKNOWLEDGEMENT

The Ministry of Education, Science and Technological Development of the Republic of Serbia supported this work under contract 171007.

AUTHORS' CONTRIBUTIONS

The idea of the paper was carried out by D. S. Arbutina and A. I. Vasić-Milovanović, the other authors participated in the concept of the instrumental and measurement of uncertainty measurements. The manuscript was conceived and written by all the authors.

REFERENCES

[1] Standler R. B., *Protection of Electronic Circuits from Overvoltages*, Dover Publications, New York, USA, 2002
[2] Beyer, M., Boeck, W., *Hochspannungstechnik, Theoretische und Praktische Grundlagen*, Springer-Verlag, Berlin, 1986
[3] Howard, C., *New Avalanche Diode for Transient Protection*, Electronic Product Design, New York, USA, 1983
[4] Vujisić, M., *et al*., Influence of Working Conditions on Over-Voltage Diode Operation, *Journal of Optoelectronics and Advanced Materials, 9* (2007), 12, pp. 3881-3884
[5] Osmokrović, P., *et al.*, Triggered Vacuum and Gas Spark Gaps, *IEEE Transactions on Power Delivery, 11* (1996), 2, pp. 858-864
[6] Jeftenić, I., *et al*., Aging of Stator Coil Interconductor Insulation of High Voltage Asynchronous Motor, *IEEE Transactions on Dielectrics and Electrical Insulation, 25* (2018), 1, pp. 352-359
[7] Osmokrović, P., *et al*., Investigation of the Optimal Method for Improvement of the Protective Characteristics of Gas-Filled Surge Arresters – With/Without the Built-In Radioactive Sources, *IEEE Transactions on Plasma Science, 30* (2020), 5, pp. 1876-1880
[8] Perazić, L., *et al*., Application of an Electronegative Gas as a Third Component of the Working Gas in the Geiger-Muellller Counter, *Nucl Technol Radiat, 33* (2018), 3, pp. 268-274
[9] Messenger, G. C., Ash, M. S., *The Effects of Radi ation on Electronic Systems*, 2nd ed., an Nostrand Reinhold, New York, USA, 1992
[10] Dekić, S., *et al.*, Conditions for the Applicability of the Geometrical Similarity Law to Impulse Breakdown in Gases, *IEEE Transactions on Dielectrics and Electrical Insulation, 17* (2010), 4, pp. 1185-1195
[11] Osmokrović, P., *et al*., Stability of the Gas Filled Surge Arresters Characteristics Under Service Conditions, I*EEE Transactions on Power Delivery, 11* (1996), 1, pp. 260-266

[12] Lazarević, Z., *et al*., A Novel Approach for Temperature Estimation in Squirrel-Cage Induction Motor Without Sensors, *IEEE Transactions on Instrumentation and Measurement, 48* (1999), 3, pp. 753-757
[13] Lazarević, D. R., *et al*., Radiation Hardness of Indium Oxide Films in the Cooper-Pair Insulator State, *Nucl Technol Radiat, 27* (2012), 1, pp. 40-43
[14] Osmokrović, P., *et al.*, The New Method of Determining Characteristics of Elements for Overvoltage Protection of Low-Voltage System, *IEEE Transactions on Instrumentation and Measurement, 55* (2006), 1, pp. 257-265
[15] Vereb, L., *et al*., Effect of Insulation Construction Bending on Stator Winding Failure, *IEEE Transactions on Dielectrics and Electrical Insulation, 14* (2007), 5, pp. 1302-1307
[16] Frigura-Iliasa, F. M., *et al*., Case Study About the Energy Absorption Capacity of Metal Oxide Varistors with Thermal Coupling, *Energies, 12* (2019), 3, 536
[17] Metwally, I. A., Heidler, F. H., Reduction of Lightning-Induced Magnetic Fields and Voltages Inside Struck Double-Layer Grid-Like Shields, *IEEE Transactions on Electromagnetic Compatibility, 50* (2008), 4, pp. 905-912
[18] Stanković, K. D., Perazić, L., Determination of Gas-Filled Surge Arresters Lifetime, *IEEE Transactions on Plasma Science, 4*7 (2019), 1, pp. 935-943
[19] Djogo, G., Osmokrović, P., Statistical Properties of Electrical Breakdown in Vacuum, *Ieee Transactions On Electrical Insulation, 24* (1989), 6, pp. 949-953.
[20] Osmokrović, P., *et al*., Radioactive Resistance of Elements for Over-Voltage Protection of Low-Voltage Systems, *Nuclear Instruments and Methods in Physics Research, Section B: Beam Interactions with Materials and Atoms, 140* (1998), 1-2, pp. 143-151
[21] Jusić, A., *et al*., Synergy of Radioactive ^{241}Am and the Effect of Hollow Cathode in Optimizing Gas-Insulated Surge Arresters Characteristics, *Nucl Technol Radiat, 33* (2018), 3, pp. 260-267
[22] Osmokrović, P., *et al*., Mechanism of Electrical Breakdown of Gases for Pressures from 10-9 to 1 bar and Inter-Electrode Gaps from 0.1 to 0.5 mm, *Plasma Sources Science and Technology, 16* (2007), 3, pp. 643-655
[23] Osmokrović, P., Electrical Breakdown of SF6 at Small Values of the Product *pd*, *IEEE Transactions on Power Delivery, 4* (1989), 4, pp. 2095-2099
[24] Vereb, L., *et al*., Effect of Insulation Construction Bending on Stator Winding Failure, *IEEE Transactions on Dielectrics and Electrical Insulation, 14* (2007), 5, pp. 1302-1307
[25] Pejović, M. M., Stanković, K., Experimental Investigation of Breakdown Voltage and Electrical Breakdown Time Delay of Commercial Gas Discharge Tubes, *Japanese Journal of Applied Physics, 50* (2011), 8R, 086001
[26] ***, The Commercial Gas-Filled Surge Arresters, https://www.streamer-electric.com/local/templates/streamer/img/main-protect/9.png
[27] Čaršimamović, A. S., *et al*., Low Frequency Electric Field Radiation Level Around High-Voltage Transmission Lines and Impact of Increased Voltage Values on the Corona Onset Voltage Gradient, *Nucl Technol Radiat, 33* (2018), 2, pp. 201-207
[28] Osmokrović, P., *et al*., The Influence of the Electric Field Shape on the Gas Breakdown Under Low Pressure and Small Inter-Electrode Gap Conditions, *IEEE Transactions on Plasma Science, 33* (2005), 5, pp. 1677-1681
[29] Osmokrović, P., *et al*., The Validity of the General Similarity Law for Electrical Breakdown of Gases, *Plasma Sources Science and Technology, 15* (2006), 4, pp. 703-713
[30] Stanković, K., Alimpijević, M., Free-Electron Gas Spectrum Uniqueness in the Mixture of Noble Gases, *Contributions to Plasma Physics, 56* (2016), 2, pp. 126-133
[31] Pejović, M. M., *et al*., Investigation of Post-Discharge Processes in Nitrogen at Low Pressure, *Physics of Plasmas, 19* (2012), 12, 123512
[32] Osmokrović, P., The Irreversibility of Dielectric Strength of Vacuum Interrupters After Short-Circuit Current Interruption, *IEEE Transactions on Power Delivery, 6* (1991), 3, pp. 1073-1080
[33] Osmokrović, P., *et al*., Determination of Pulse Tolerable Voltage in Gas-Insulated Systems, *Japanese Journal of Applied Physics, 47* (2008), 12, pp. 8928-8934
[34] Saranya, A., *et al*., Role of Hexamine in ZnO Morphologies at Different Growth Temperature with Potential Application in Dye Sensitized Solar Cell, *Materials Science in Semiconductor Processing, 92* (2019), pp. 108-115
[35] Osmokrović, P., *et al*., Reliability of Three-Electrode Spark Gaps, *Plasma Devices and Operations, 16* (2008), 4, pp. 235-245
[36] Osmokrović, P., *et al*., Numerical and Experimental Design of Three-Electrode Spark Gap for Synthetic Test Circuits, *IEEE Transactions on Power Delivery, 9* (1994), 3, pp. 1444-1450
[37] Vujisić, M., *et al*., Radiataion Effects in Polycarbonate Capacitors, *Nucl Technol Radiat, 24* (2009), 3, pp. 157-218
[38] Osmokrović, P., *et al*., Influence of the Electrode Parameters on Pulse Shape Characteristic of Gas-Filled Surge Arresters at Small Pressure and Inter-Electrode Gap Values, *IEEE Transactions on Plasma Science, 33* (2005), 5, pp. 1729-1735
[39] Nedić, T., *et al*., Efficient replacement of the Radioactive Sources in the Gas-Filled Surge Arresters Construction for the Insulation Co-Ordination at the Low Voltage Level, *Nucl Technol Radiat, 35* (2020), 2, pp. 130-137
[40] ***, BIPM, IEC, IFCC, ISO, IUPAC, IUPAP and OIML: Guide to the Expression of Uncertainty in Measurement, Geneva, Switzerland: International Organization for Standardization, 1995

Received on November 17, 2020
Accepted on November 27, 2020

Далибор С. АРБУТИНА, Александра И. ВАСИЋ-МИЛОВАНОВИЋ, Теодора М. НЕДИЋ, Ацо Ј. ЈАНИЋИЈЕВИЋ, Љубинко Б. ТИМОТИЈЕВИЋ

МОГУЋНОСТ ПОСТИЗАЊА ПРИХВАТЉИВЕ БРЗИНЕ ОДЗИВА ГАСНИХ ОДВОДНИКА ПРЕНАПОНА СУПСТИТУЦИЈОМ АЛФА ИЗВОРА ЗРАЧЕЊА ИЗБОРОМ МАТЕРИЈАЛА ЕЛЕКТРОДА И ТОПОГРАФИЈОМ ЊИХОВИХ ПОВРШИНА

У раду се разматра могућност супституције примене радиоактивног α-извора за побољшање карактеристика гасног одводника пренапона. Решење овог проблема се тражи у инжењерингу карактеристика применом различитих материјала електрода и различитих топографија електродних површина. Испитивани су материјали који се разликују по вредности излазног рада. Топографије електродних површина су биле или полиране, или са угравираним правилним шиљцима, или са шупљинама. Рад је претежно експерименталног карактера. Експерименти су вршени под добро контролисаним лабораторијским условима. Мерна несигурност експерименталног поступка је била задовољавајућа. Експериментални резултати показују да је могуће избећи уградњу радиоактивног извора у гасне одводнике пренапона и како то треба. На тај начин би се избегле могуће контаминације природне средине веома опасним α – радиоактивним изворима.

Кључне речи: гасни одводник пренапона, ко-ординација изолације, нисконапонски ниво